SENSOR NON-DESTRUCTIVE OF ESTIMATION OF SURFASES IN VACUUM

E.A. Deulin, A.V. Skrylev, M.S. Basmanov
Bauman Moscow State Technical University, MT-11, 2nd Baumanskaia st., 5, Moscow,105005, Russia,
deulin@bmstu.ru, skrylev_av@mail.ru

I. INTRODUCTION

The idea to create a new vacuum sensor for measurement of residual pressure in wide pressure range appeared as a result of study of the "dry friction" phenomenon. We use many different types of vacuum or residual pressure sensors (gauges) at present time: Bourdon tube, thermocouple vacuum gauge, ion vacuum gauge, cold cathode gauge, Bayard Alpert etc. Nevertheless, no type of sensor can be used at present time to measure a residual pressure and a surface coverage coefficient simultaneously. The presented sensor is based on functional dependence of friction coefficient on residual pressure as well as on coverage coefficient [2, 10].

II. ANALYSIS OF EMPIRICAL AND THEORETICAL RESULTS

The functional dependence of so called "dry friction" coefficient on the residual pressure in "vacuum" exists both for metal-metal friction pairs [10] and for dielectric-dielectric friction pairs [4, 5]. The experiments show that the mentioned functional dependence exists in the case of ball bearing run in vacuum too [3].

The summary diagram illustrating the mentioned functional dependence is shown in Fig. 1, 2.

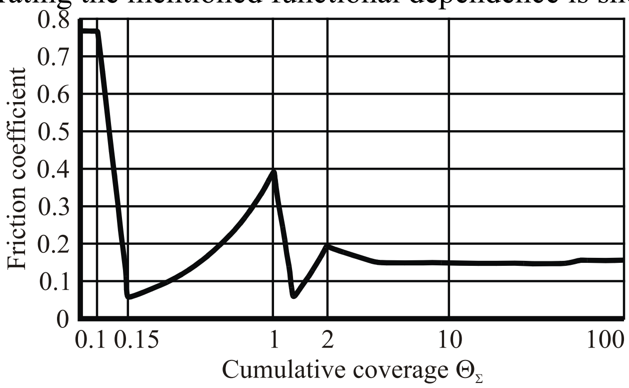

Fig. 1. Variation of theoretical value of friction coefficient for Si – Si friction pair (silicon monocrystal friction pair) versus cumulative coverage.

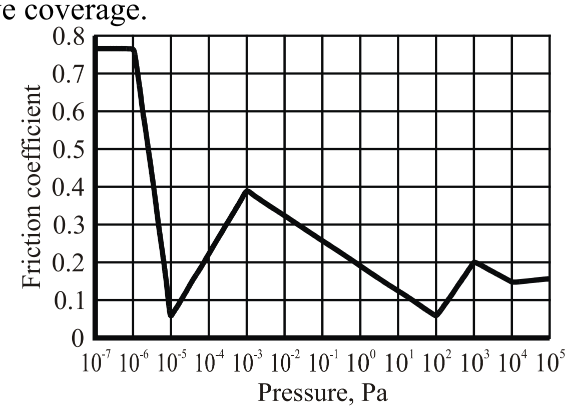

Fig. 2. Variation of theoretical value of friction coefficient for Si – Si friction pair (silicon monocrystal friction pair) versus residual pressure.

The experimental results [4, 5] presented in Fig. 3 – 5 are in good agreement with the results [2] of analysis implemented for the sample of the same surface geometry as used in [4]. Different types of vacuum sensors were used for the experiments. German made sensors

were used
to obtain the earlier published results [5]: 1) DVR – VACUUMBRAND (10^5 – 10^{2} Pa); 2) CTR90, Leybold Co, (10^{4} – 10^{-0} Pa); 3) CTR91, Leybold Co, (10^{2} – 10^{-2} Pa), ion gauge (10^{0}- 10^{-4} Pa); 4) Bayard-Alpert sensor. The previous experimental results [4] were obtained using Russian (USSR) made analogue sensors. The results show, that "dry" friction is a complex phenomenon. It depends mainly on coverage
of the surface and on the surface geometry as well as sorption energy.

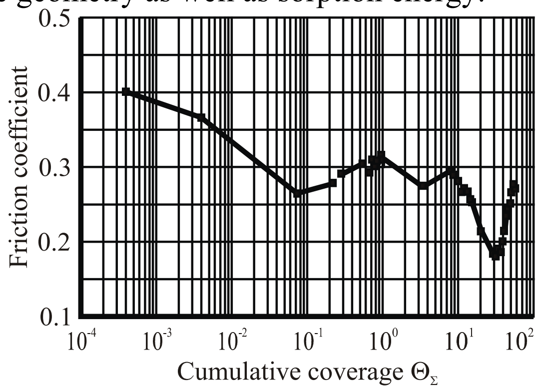

Fig. 3. Variation of empirical value of friction coefficient for Si – Si friction pair (silicon monocrystal friction pair) versus cumulative coverage.

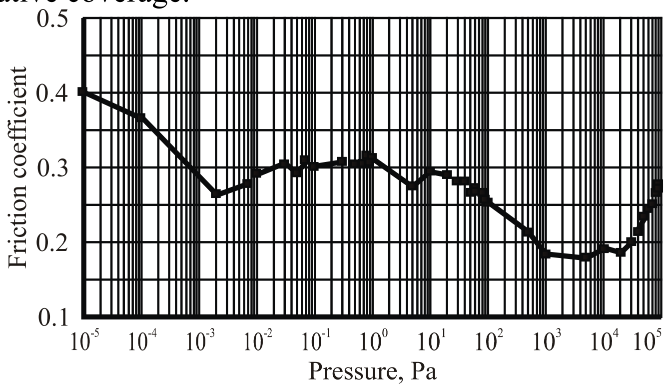

Fig. 4. Variation of empirical value of friction coefficient for Si – Si friction pair (silicon monocrystal friction pair) versus residual pressure.

It was shown theoretically [2, 10], that the characteristic parameter of "dry friction" is coverage coefficient Θ_Σ which depends mainly on sorbed water. Dry friction is a complex phenomenon which includes four different components. Capillary component has an effect in low and middle vacuum (at cumulative coverage more than 2). Viscose component prevails in low, middle and in high vacuum (at cumulative coverage less 2). Adhesive component is determinative in high and ultra high vacuum (at $2 > \Theta_\Sigma > \Theta_{\Sigma CH}$). Cohesive component comes into play in extremely high vacuum in case of smooth surfaces ($\Theta_\Sigma < \Theta_{\Sigma CH}$). Cohesive component has an influence on friction to some extent at any pressure in case of real "rough" surfaces.

As illustrated in diagrams (Fig. 1 – 5) friction coefficient has four maximums:

1. At Θ_Σ = 20…150 ($\Theta_\Sigma = \Theta_{max}$). It is caused by the largest contact area, that is close to geometrically determined nominal contact area.
2. At Θ_Σ = 2. It is governed by the maximal value of viscous friction gradient in the "quasi-liquid" part of the cumulative coverage.
3. At Θ_Σ = 1. Where the largest contact area of the smooth surface is covered with a sorbed gas.
4. At $\Theta_\Sigma < (N+F_{CHN})/(\sigma_B \cdot A \cdot P^4(X))$. It is explained with the largest (cohesive) attraction energy (energy of friction) in contact areas.

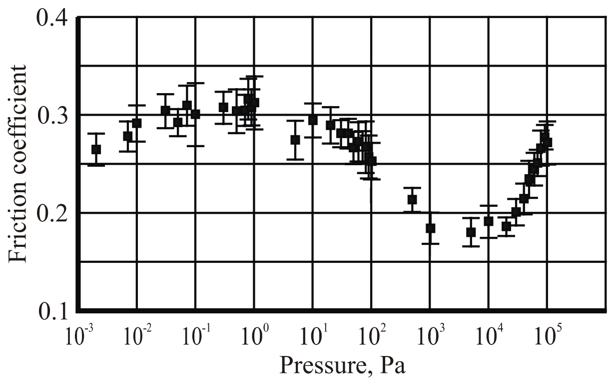

Fig. 5. Variation of empirical value of friction coefficient for Si – Si friction pair (silicon monocrystal friction pair) versus residual pressure (in limited pressure range within the error span).

The theoretical graphs of different components of friction coefficient (viscous, capillary, adhesion and cohesion components) are shown in Fig. 6 as functions of coverage coefficient for Si – Si friction pair with polished surfaces.

The listed above maxima of the cumulative friction coefficient take shape over summation of graphs of different friction components in different ranges of coverage coefficient variation. The fourth maximum is not shown in Fig. 6 for cumulative friction coefficient because the capillary component is difficult to calculate for a polished Si – Si friction pair. The graph of the cumulative friction coefficient in Fig. 6 fits well with the graphs shown in Fig. 1, 3.

Coverage coefficient Θ depends on residual pressure according to BET equation (1) [1]:

$$\Theta = e^{\frac{E_S - E_L}{R \cdot T}} \cdot P \cdot \left\{ (P_S - P) \cdot \left[1 + \left(e^{\frac{E_S - E_L}{R \cdot T}} - 1 \right) \cdot \frac{P}{P_S} \right] \right\}^{-1}, \quad (1)$$

where P is a residual pressure measured in slot between sliding surfaces, Pa; P_S is a measured saturated gas pressure, Pa; E_S, E_L are adsorption heat and heat of vaporization for the gas which residual pressure is being measured by the sensor, J; R is the absolute gas constant; T is a gas (surface) temperature, K.

Recalculation of empirical data published by different authors [3-6, 9] into coordinates “friction coefficient – residual pressure” “friction coefficient – temperature”, “friction coefficient – humidity” demonstrates the similarity of their empirical results to the theoretical values shown in coordinates “friction coefficient - coverage” (Fig.1, 3).

So, for example, the diagram in Fig. 7 represents the original results [6] (before recalculation) for SiO_2 - SiO_2 friction depending on temperature at relative humidity of 40 … 60 % and the diagram in Fig. 8 represents the same results recalculated in coordinates “friction coefficient – coverage”.

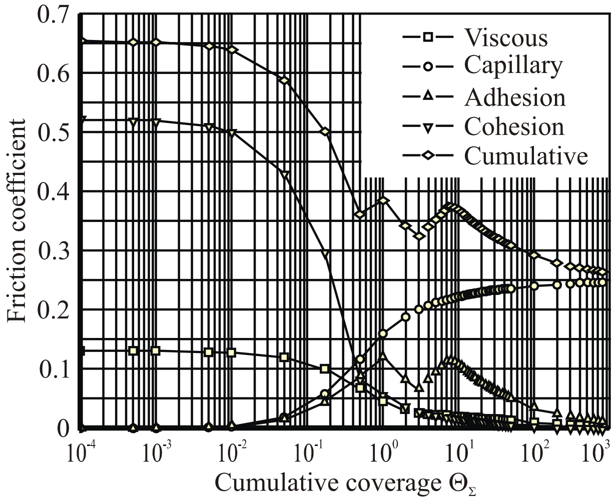

Fig. 6. Diagram of theoretical value of friction coefficient depending on cumulative coverage coefficient Θ_Σ (upper curve), that is a sum of the underlying curves (viscous, capillary, adhesive, cohesive friction components [2, 10]).

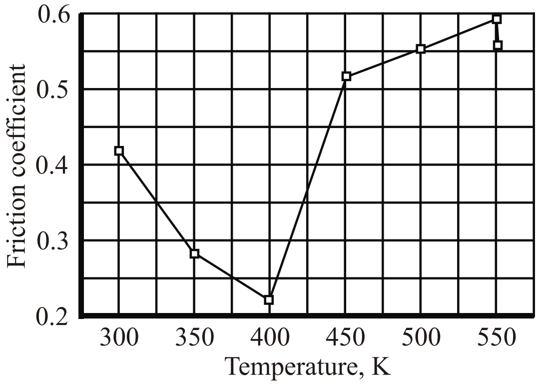

Fig. 7. Original empirical values of $SiO_2 - SiO_2$ friction coefficient at different temperatures [6]. empirical values of $SiO_2 - SiO_2$ friction coefficient.

The obtained theoretical values conform to the empirical values shown in Fig. 3 good enough.

The empirical values of “Si – Si” friction coefficient depending on relative humidity *RH* [9] shown in Fig. 9 can be considered from the position of unity of differently presented friction phenomena. This might seem, that the values presented in Fig. 9 are not related with the values in Fig. 1 and in Fig. 3. But, the analysis of coverage coefficient gives us in Fig. 10, that these values coincide with the result in Fig. 1 and 3 (see the right part of the diagram for the zone of $\Theta_\Sigma = 8 \ldots 700$ monolayers).

Thus the values obtained by different authors at different environmental conditions (*P*, *T*, *RH*) are very similar to each other if presented as a function of coverage coefficient.

As it was demonstrated above and theoretically shown in [2, 10] the experimental results obtained at various residual pressures [4, 5], temperatures [6], and relative humidity values [9] allow interconversion and can be expressed as a function of coverage coefficient (see Fig. 11). This conclusion about unity of “different” friction phenomena is confirmed by recalculation of empirical data according to the presented theory [2, 10].

The observed phenomenon of dependence of friction coefficient on coverage coefficient can be utilised in a new vacuum sensor to measure a residual pressure and a coverage coefficient at the same time.

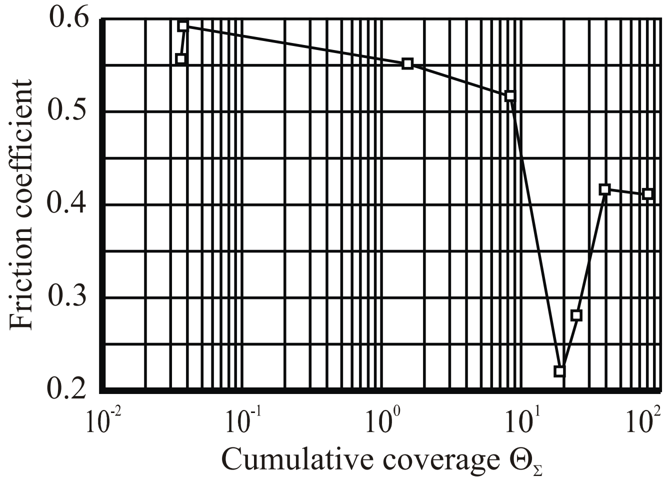

Fig. 8. Empirical values of SiO_2 – SiO_2 friction coefficient recalculated to coordinates “friction coefficient – coverage”.

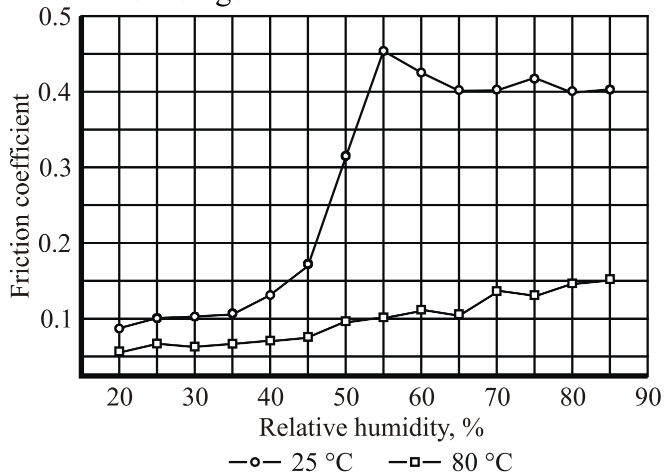

Fig. 9. Empirical hydrophilic Si – Si friction coefficient at various relative humidity [9] at t = 25 °C (upper graph), t = 80 °C (lower graph).

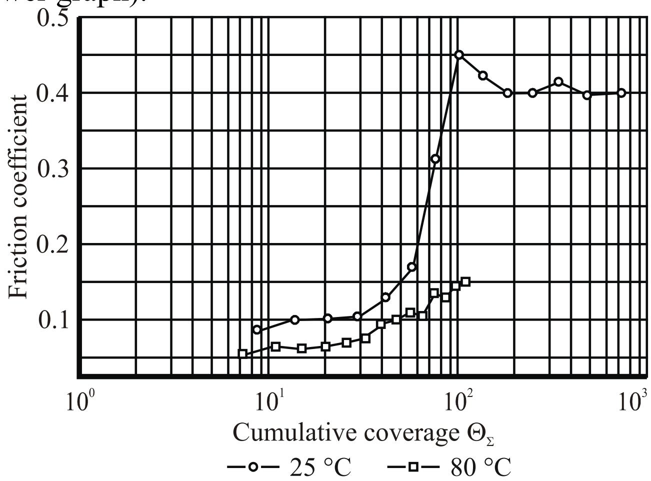

Fig. 10. Empirical hydrophilic Si – Si friction coefficient recalculated into coordinates “friction coefficient – coverage”.

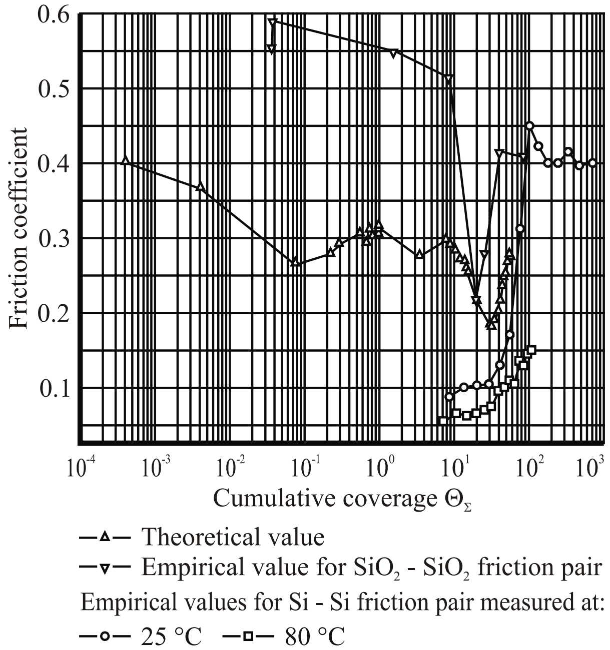

Fig. 11. Diagrams built by empirical data [4-6, 9] recalculated into coordinates "friction coefficient – coverage".

III. A Proposed Sensor Design

We have shown the unity of "different" friction phenomena, and the opportunity to utilise the theoretical and empirical dependencies in design of a new sensor [7, 8] for simultaneous residual pressure (vacuum) and coverage coefficient measurements. The proposed scheme of such sensor is shown in Fig. 6 and 7.

The main elements of the sensor (see Fig. 12) are rubbing rings 12 and 11, which are joined correspondingly with driving (pos. 2, 4) and "measuring" (pos 5, 9, 10) parts of the presented sensor. Ring 11 is flat with the "window hole" to allow a penetration of residual gases and their sorption on "sliding surface" of the ring 12. The "angular" part of the "window" is following:

$$\varphi = \frac{L}{\pi \cdot D} = \frac{V \cdot N_{1s} \cdot 4 \cdot k \cdot T}{P_c \cdot V \cdot \alpha \cdot \pi \cdot D} = \frac{N_{1s} \cdot k \cdot T}{1.5 \cdot 10^3 \cdot V_a \cdot \alpha},$$

$$V = \frac{10^{-4} \cdot V_a \cdot \alpha \cdot L}{N_{1s} \cdot 4 \cdot k \cdot T}, \qquad (2)$$

[m/s]

$$L = \frac{V \cdot N_{1s} \cdot 4 \cdot k \cdot T}{P_c \cdot V_a \cdot \alpha}, \qquad [m]$$

where V is sliding velocity corresponding to forming of the sorbed gas layer on a sliding surface of ring 12; V_a is an average velocity of thermal movement of gas molecules retained on the surfaces in vacuum; D is a mean diameter of race; L is a length of the window; N_{1s} is a number of molecules sorbed on the unit square of the surface; T is a surface temperature, K; α is an adhesion coefficient; P_c is a "critical" residual pressure being measured, it correspond to $P_c \approx 10^{-4}$ Pa in our case or to $\Theta_\Sigma = 1$ (close to the "boundary" between high vacuum and UHV).

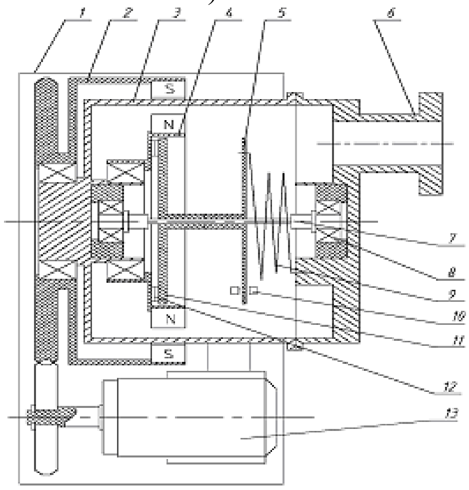

Fig. 12. The first scheme of ultra wide range vacuum sensor [7] is based on Si-Si friction pair: 1 is a screen, 2 is a rotating magnet drive, 3 is a case, 4 is a rotor, 5 is a measuring rotor, 6 is a vacuum flange, 7 is a shaft, 8 is a supporting ball bearing, 9 is a torsion for measuring torque, 10 is an optron sensor, 11 is the first rubbing ring, 12 is the second rubbing ring, 13 is a driving motor.

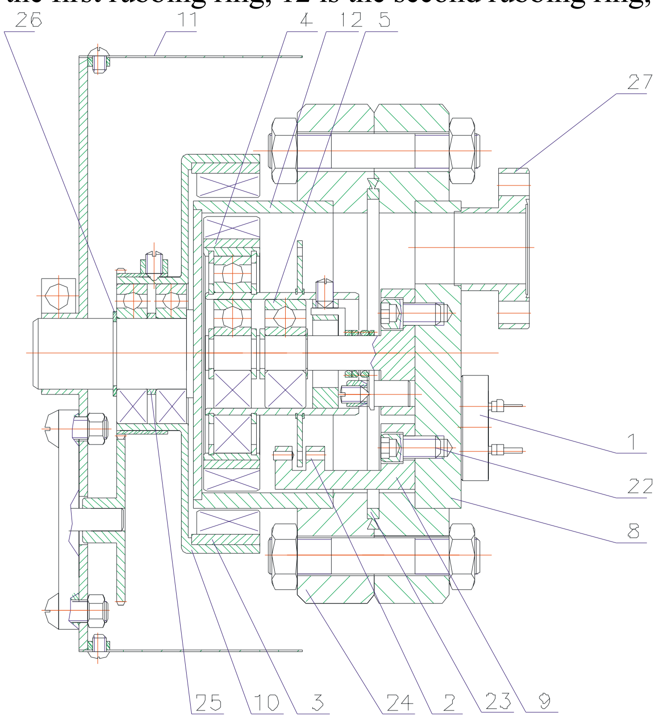

Fig. 13. The second scheme of vacuum sensor for ultra wide measurement range [3, 8]: 1 are torque measurement feedthroughs; 2 is a torque photon-coupled pair; 3, 10 is a rotating magnet drive; 8, 9, 11, 12 is a case; 4 is a measuring ball bearing (is tested); 5 are supporting ball bearings; 25 is a rotor; 26 is a shaft; 27 is a vacuum flange.

The main elements of the second version of the sensor (Fig. 13) are measuring ball bearing 4 (is tested), the torque on which is measured, rotating magnet drive 3, 10, and the torque photon-coupled pair (pos. 2). Torsion spring is not shown in Fig. 12. Basic dimensions of the sensor are similar to ordinary ion-gauge sensor dimensions. Other versions of the new sensor are being patented now.

IV. Conclusion

1. The results of experimental studies of “dry friction” at various residual pressures, temperatures, and humidity values allow interconversion and can be expressed as a function of coverage coefficient.
2. Unity of “different” friction phenomena gives the opportunity to create the new vacuum sensor for taking measurements of residual pressure and coverage coefficient.

Acknowledgments

Authors thank Russian Ministry of Education for financial support of this research with Grant №П2421. Authors also would like to thank for productive discussion of the experimental results, as well as former BMSTU students, DSc. A. Gatsenko, DSc. Tsukuba, Ibaraki, and BMSTU students I. Gladyshev, E. Tkacheva for the excellent experiment results and for the interesting results of theoretical analysis.

References

[1] Brunauer, S., P.H. Emmett, and E. Teller, Adsorption of Gases in Multimolecular Layers. *Journal of the American Chemical Society*, 1938. **60**(2): p. 309-319.

[2] Deulin, E.A. The Role of Adsorbed Water Film For Sliding Friction of Smooth and Rough Surfaces. in *Tribology - Science and Application Conference*. 2004. Vienna.

[3] Deulin, E.A., et al. Effect of Gas Adsorption on Tribology of Ball Bearings in Vacuum. in *15th International Colloquium on Tribology "Automotive and Industrial Lubrication"*. 2006. Stuttgart, Ostfildern: Technische Academie Esslingen.

[4] Deulin, E.A., A.A. Gatsenko, and A.B. Loginov, Friction force of smooth surfaces of SiO_2–SiO_2 as a function of residual pressure. *Surface Science*, 1999. 433-435: p. 288-292.

[5] Deulin, E.A., A.A. Gatsenko, and P. Repa, Friction coefficient variation of smooth surfaces in vacuum in *9th Joint Vacuum Conf*. 2002: Schloss Seggau, Austria. p. 20.

[6] Deulin, E.A. and I.V. Gladyshev, Residual pressure and temperature influence on SIO_2-SIO_2 friction coefficient, in *Nordtrib*. 2002. p. 176.

[7] Patent of RF № 2316744. Deulin, E.A. *A method of vacuum measurement*. Bull. Inv.-10.02, 2008.

[8] Patent of RF № 2263886. Deulin, E.A., et. al. Friction Vacuum Gauge. Bull. Inv.-10.11, 2005.

[9] Scherge, M., X. Li, and J.A. Schaefer, The effect of water on friction of MEMS. *Tribology Letters*, 1999. **6**(3-4): p. 215-220.

[10] Деулин, Е.А., ed. *Механика и физика точных вакуумных механизмов*. Vol. 1. 2001, Владимирский государственный университет: Владимир. In Russian.